Comparative Analysis of Embankment Slope Stability using Geofoam

Arsila Hairunnisa, Eddy Triyanto Sudjatmiko*

Department of Civil Engineering, President University, Cikarang, Indonesia

Received 30 March 2025; received in revised form 06 April 2025; accepted 07 April 2025

Abstract

Landslides caused by land movement due to unstable soil are one of the causes of infrastructure damage such as cracks or collapse and can pose various threats to humans. The development of technology in geotechnics called geofoam material, which is also known as lightweight material can be a solution. This study aims to determine whether geofoam can be used as a partial replacement material for soil by comparing the results that have been analyzed using Plaxis 2D software. Landslides with existing silt clay soil conditions occur because the safety factor is 1 in undrained conditions. Meanwhile, on embankment soil built with geofoam measuring 1 x 4 m on a 15 m thick embankment and a slope of 1:2, it shows that the safety factor on the slope increases to 1.5 for undrained conditions and 1.9 for drained conditions. A reduction in the amount of geofoam by 37% was carried out and the SF figures were 1.34 for undrained and 1.6 for drained. These results met the requirements of SNI 8460:2017, where SF>1.25 and external load of 25 kN/m^2 did not change the safety factor on the geofoam embankment. The results of the effective stress distribution pattern and shear strain showed that the activity that occurred on the embankment with geofoam was very low compared to the existing soil. It can be concluded that geofoam material can replace part of the embankment, because it has been proven to be able to stabilize the slope on the embankment.

Keywords: geofoam, landslide, safety factors, silty clay, stabilize the slope

1. Introduction

Landslides are a problem of soil stability that often occurs due to the lack of soil strength to withstand the load. Based on data from BNPB (National Disaster Management Agency) in 2023, 591 cases of landslides were recorded in Indonesia, with West Java Province ranking the highest at 185 cases as reported by Badan Pusat Statistik in 2024. Topographically, the West Java Province has many steep slopes, making this area prone to landslides (Fig. 1).

Landslide caused by soil displacement due to unstable soil is one of the causes of infrastructure damage, such as cracking or the sinking of one side, and it can pose various threats to humans. The addition of supplementary materials such as cement and limestone powder are some options to improve the CBR (California Bearing Ratio) strength of subgrade soil. However, this method is sometimes inefficient because it requires additional time to process these materials to ensure they are properly mixed with the soil [1]. In addition, the steep slope conditions in line with West Java's topography and the silty clay soil type have a high potential for landslides.

As a solution, currently, human-made technology in the field of geotechnics called geosynthetics has been developed to enhance soil stability. One common type of geosynthetics used for soil reinforcement and stabilization is geofoam. With its advantage of weighing only 0.6-2.6% of the weight of embankment soil, ease of application, and being unaffected by time and

* Corresponding author. E-mail address: eddy.triyanto@president.ac.id
Tel.: +62(0)21 89109763

weather conditions, this material proves to be a suitable solution [2].

To ensure the effectiveness of embankment stabilization using geofoam, this study uses analysis software such as Plaxis to compare displacement between soil embankment and embankment with geofoam. This involves evaluating the effectiveness of soil resistance by comparing the stability of soil embankments based on the thickness of the geofoam layer [3-6] and embankments without using the material geofoam.

Fig 1. Crown landslide estimation by google earth

2. Material and Method

This study was conducted using the following data: material layer profile, geofoam profile, and soil layer depth collected by the field investigation method planned construction of embankment project in East Karawang, West Java. Field investigation has been carried out in the form of SPT (Standard Penetration Test). For the layer (1) with silty clay type or areas where the landslides occur, there is no SPT value due to the parameters are formed from the results of trial and error in landslide (value of safety factor = 1).

Table 1 SPT value

Layer	Soil type	Soil behavior	Depth (m)	N value	Cu
2	Silty clay	Clay	0 – 15	10	40
3	Silty clay	Clay	15 <	20	128

Then for calculation, several parameters need to calculate from the SPT data (Table 1):

1) Modulus of elasticity

   Measurement of the modulus of elasticity can use the results of the Pressuremeter test in the form of a slope curve during the test. In addition, it can also be determined through the cavity expansion theory of soil properties to calculate the modulus of elasticity from the test data [7-9]. For the value of the modulus of elasticity based on the N value. The soil in this case is Silty Clay soil [10].

   a) Silty clay (2)

   $$E = 250\ Cu = \sim 10000\ kN/m^2$$

   b) Silty clay (3)

   $$E = 250\ Cu = \sim 32000\ kN/m^2$$

2) Poisson's ratio

To determine Poisson's ratio, it can be seen in Table 2 below. The soil category is medium clay. So, the value of Poisson's ratio is around 0.2 – 0.5.

Table 2 Poisson's ratio representative value [11]

Soil	μ
Loose sand	0.2 – 0.4
Medium sand	0.25 – 0.4
Dense sand	0.3 – 0.45
Silty sand	0.2 – 0.4
Soft clay	0.15 – 0.25
Medium clay	0.2 – 0.5

3) Unit weight

Based on [12], the value of unit weight for each category as shown in Table 3.

Table 3 Correlation between SPT-N value and unit weight

SPT N	0 to 4	4 to 10	10 to 30	30 to 50	> 50
Unit weight	< 15.7	14.9 to 19.6	17.3 to 20.4	17.3 to 22	> 20.4

4) Permeability

According to Table 4, since the type of soil is silty clay, the value of permeability will be lower than 1.00E-09.

Table 4 Correlation between N-value and permeability by Terzaghi in 1943

Soil	k (cm/s)	k (m/s)
Clean gravel	100 – 1	1 – 0.01
Coarse sand	1 – 0.01	0.01 – 0.0001
Fine sand	0.01 – 0.001	0.0001 – 0.000001
Silty clay	0.001 – 0.00001	0.000001 – 0.0000001
Clay	< 0.000001	0.00000001

5) Cohesion and angle friction

For correlation between cohesion and SPT-N value will be from the graphic Fig 2.

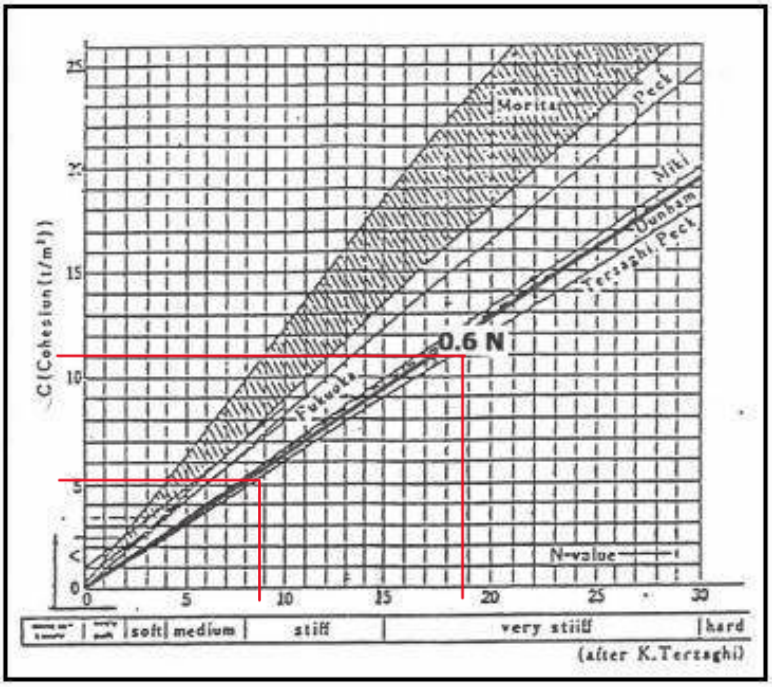

Fig. 2 Correlation between cohesion and SPT N-value by Terzaghi in 1943

Table 5 Geofoam EPS density

Type	Minimum Density (kg/m^3)
EPS 12	11.2
EPS 15	14.4
EPS 19	18.4
EPS 22	21.6
EPS 29	28.8
EPS 39	38.4
EPS 46	45.7

Table 6 Common dimension of EPS

Dimension	(mm)
Width	305 to 1219
Length	1219 to 4877
Thickness	25 to 1219

For geofoam material, the density and common dimension from ASTM C-578 (see Table 5 and Table 6). The parameters were obtained from field data, except for the Poisson's ratio parameter, trial and error experiments were carried out until landslide conditions were achieved on existing soil or SF value is 1. All parameters obtained are in Table 7.

For traffic load, it is according to SNI 8460:2017, the load is 15 kPa as the load on the traffic load and 10 kPa as the dead load from the surrounding structure. The total distributed load in the modelling is 25 kPa According to SNI 8460:2017, the load is 15 kPa as the load on the traffic load and 10 kPa as the dead load from the surrounding structure. The total distributed load in the modelling is 25 kPa.

Table 7 Material parameters for soil and embankment

No.	Parameter	Symbol	Silty clay (1)	Silty clay (2)	Silty clay (3)	Geofoam (1 x 4 m)
Depth (m)			0 - 7	0 - 7	> 15	
1	Material		Mohr Coulomb			Linear elastic
2	The type of material behavior		Undrained/ Drained			Non-porous
3	Unit weight saturated (kN/m^3)	γ_{sat}	16	17	18	-
4	Unit weight unsaturated (kN/m^3)	γ_{unsat}	16	17	18	0.22
5	Permeability X (m/s)	kx	2.00E-09	2.00E-09	2.00E-09	-
6	Permeability Y (m/s)	ky	1.00E-09	1.00E-09	1.00E-09	-
7	Young Modulus (kN/m^2)	E	1764	8400	26880	5000
8	Poisson's ratio	v	0.35	0.35	0.35	0.05
9	Cohesion (kN/m^2)	c'	2	6	12	-
10	Angle friction (°)	Φ	12	18	22	-

To measure the structure is safe or not, SNI 8460:2017 has design criteria. Consideration to the loads that will be received by the excavation and embankment slopes is 10 kPa for dead load of structure. As for traffic loads according to SNI 8460:2017, they are lister in Table 8. Also, for safety factor criteria of soil slope stability based on SNI 8460:2017 in Table 9.

Table 8 Traffic load

Road Type	Traffic Load (kPa)	Other Load /Environment (kPa)
I	15	10
II	12	10
III	12	10

Table 9 Safety factor for soil slope

Costs and consequences of slope failure	The level of uncertainty of the analysis conditions	
	Low	High
The cost of repair is comparable to the additional cost of designing a more conservative slope	1.25	1.5
The cost of repairs outweighs the additional cost of designing a more conservative slope	1.5	2.0 or more

To calculate the stability soil, Plaxis Computer Program (Finite Element Code for Soil and Rock Analysis) can be used. This program is based on Finite Element Method modelling and post-processing program capable of analyzing geotechnical problems, providing various engineering analyses regarding displacement, soil stresses, and more in geological and civil engineering planning. The program is designed to create geometries for analysis [13-16]. Plaxis Input includes parameters and geometry that will be used in the analysis. There are also various types of materials that can be used such as soil and interface, plate, geotextile, anchor, and tunnel that can be easily formed. In addition, there is also a determination of groundwater level and generated mesh in this program.

For this research, there are two conditions that affect the calculation, drained analysis and undrained analysis. Drained conditions are ideal for soils with high permeability, such as sandy soils, or soils that experience very slow loading, as well as for stimulating long-term soil behavior. In the PLAXIS 2D program, the Drained condition is used to specify that there should be no increase in Porewater Pressure on the soil material. Meanwhile, undrained soils have low permeability, such as clay, and when excess pore water pressure is applied, it does not dissipate or flow immediately. The PLAXIS 2D program's undrained conditions are used to control the rise in excess pore water pressure in soil materials.

Before doing the calculation, geometry of each model must be created, as shown in following figures.

1) Soil embankment

This model has a slope of 1:3.5 (silty clay (1) layer) as seen in Fig 3.

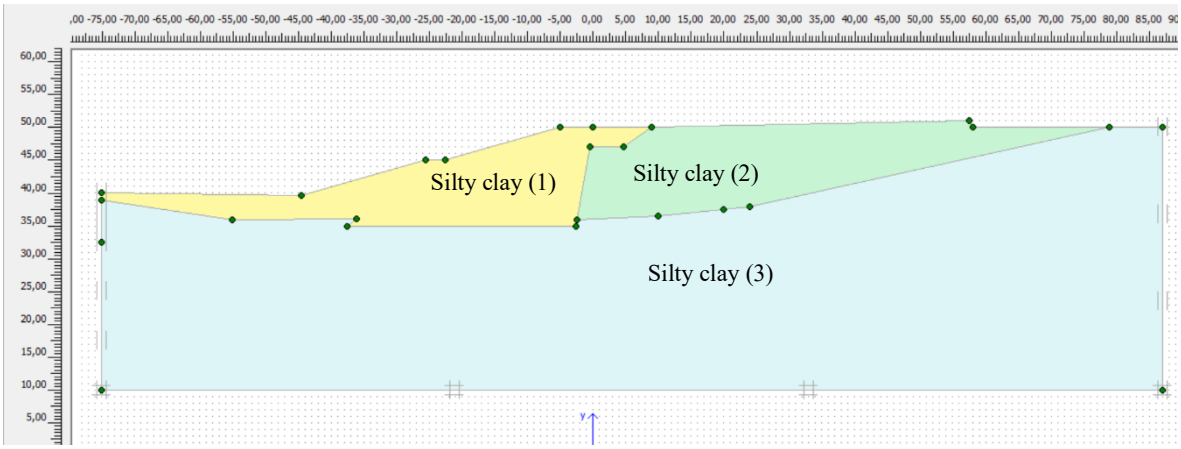

Fig. 3 Soil embankment model

2) Soil with geofoam embankment [17-21]

This model has a slope of 1:2 in both of side, with 98 pieces of geofoam and dimensions of 1x4 m as shown in Fig. 4.

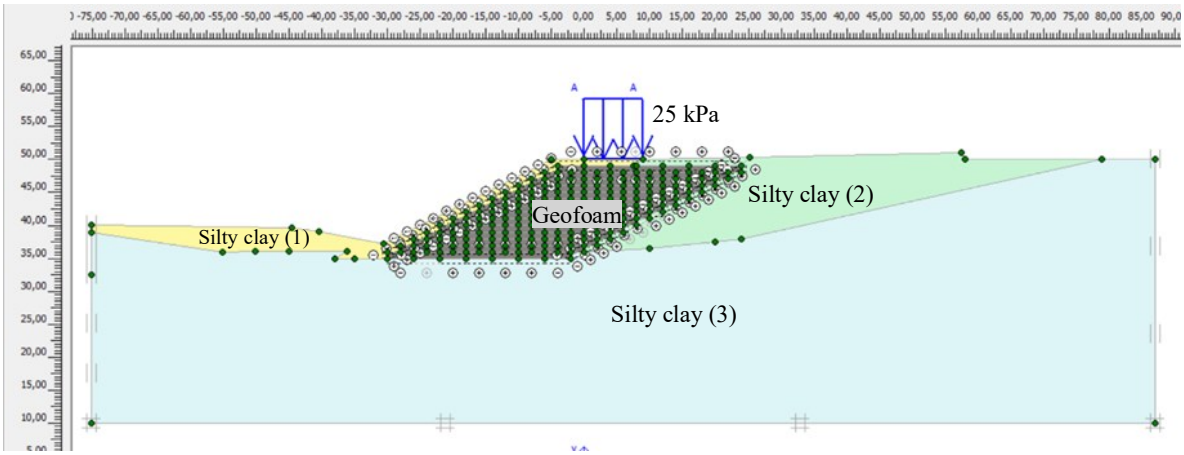

Fig. 4 Soil with geofoam embankment model

3) Soil with reduced embankment

To reduce the cost, a trial calculation of safety factors will be carried out by reducing the amount of geofoam by 37%. This model has a slope of 1:2 for the left slope and 2:1 for the right slope because the adjustment of the slope of the right slope has a value that is close to the same as the slope in the existing soil model. The number of geofoams is 60 pieces with dimensions of 1x4 m, and some of the geofoam on the right side is adjusted in length by cutting the geofoam. Shown in Fig. 5.

The variables can be seen in Table 7. By using Plaxis 2D, the output of analysis data of calculation result, such as: total settlement, effective stress, safety factors, and total displacement. The steps of this study are shown in the study methodology (Fig. 6).

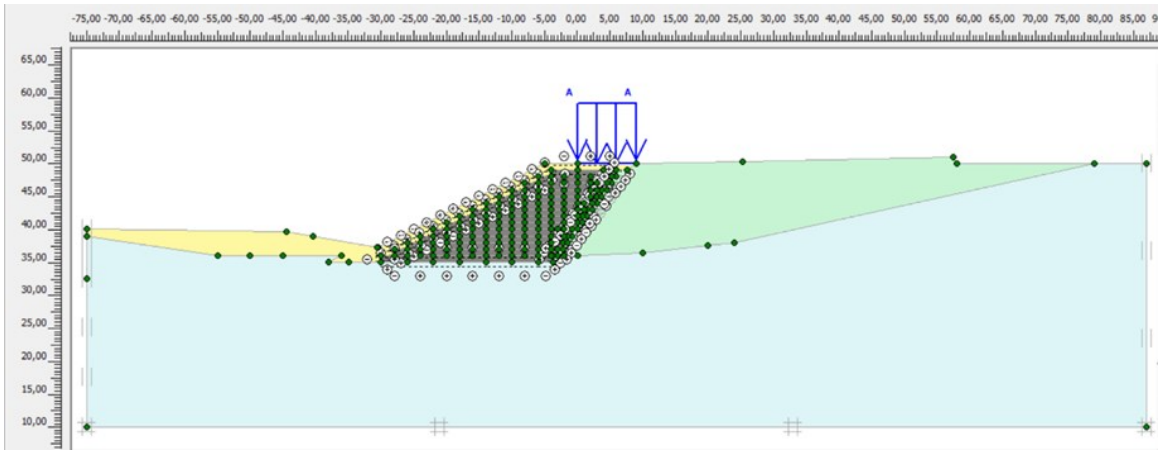

Fig. 5 Soil with reduced geofoam embankment model

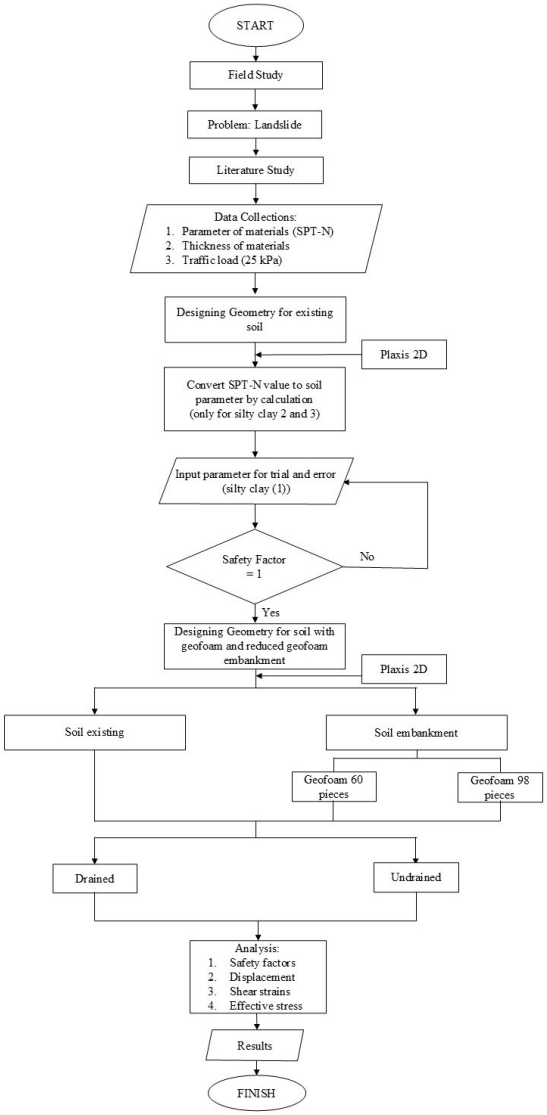

Fig. 6 Study methodology

3. Results and Discussion

3.1 Safety factors

Referring to SNI 8460:2017, the minimum requirement for safety factors is 1.25. This means that if there is a number below that number, the slope structure is not adequate. For existing soil embankment, the safety factor number (Fig. 7) the existing soil has a value of 1 in undrained conditions and 1.06 in drained conditions. Undrained conditions have a smaller value because the pore water in the soil cannot fully exit when loading occurs, thus reducing the work of effective stress (the difference between total stress and pore water stress). Because the condition SF = 1, it can be concluded that a landslide occurred in existing soil with these soil parameters.

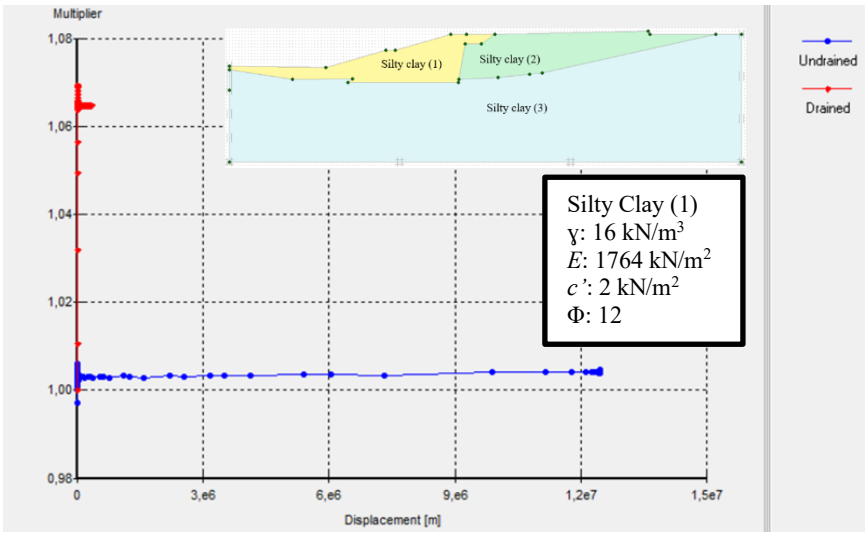

Fig. 7 Safety factors of existing soil embankment

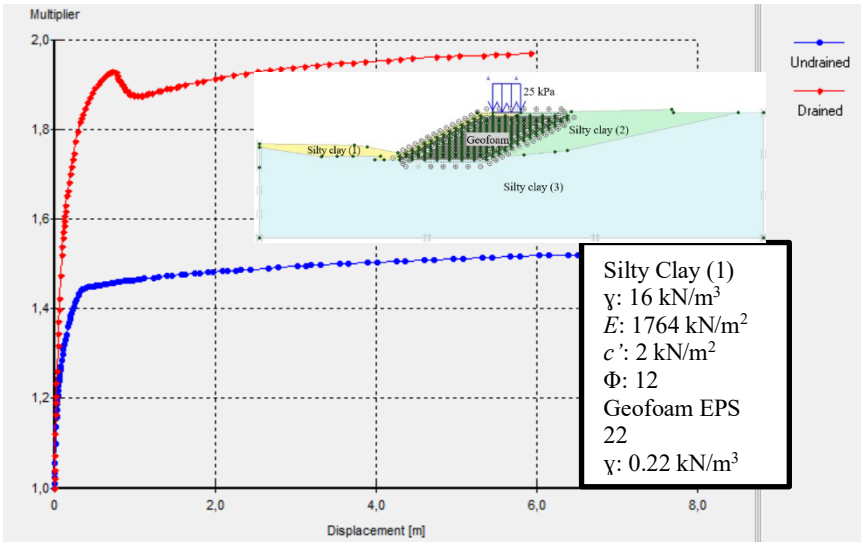

Fig. 8 Safety factors of soil with geofoam embankment

Different result of soil with geofoam embankment, geofoam have a big impact to increase the safety factor number. By arranging geofoams like bricks withstand the shear strength of the soil, also the weight of geofoam is lighter than the soil so it can decrease the load. Shown in Fig. 8 which shows that in undrained conditions, the safety factor value is 1.5 and in drained conditions it increases to 1.9. This can happen because in undrained conditions, pore water pressure tends to be greater than in

drained conditions so that the effective stress becomes smaller. According to SNI 8460:2017, there is an external loading of 15 kPa from traffic and 10 kPa from the structural roads.

The graphics in Fig. 9 show there is no significant change in safety factor number. To make the budget more efficient, reducing the amount of geofoam (37%) can be done as shown in Fig. 10. The result of safety factors for this model are 1.34 for undrained condition and 1.6 for drained condition. Both of these values are higher than the rules by SNI (SF > 1.25).

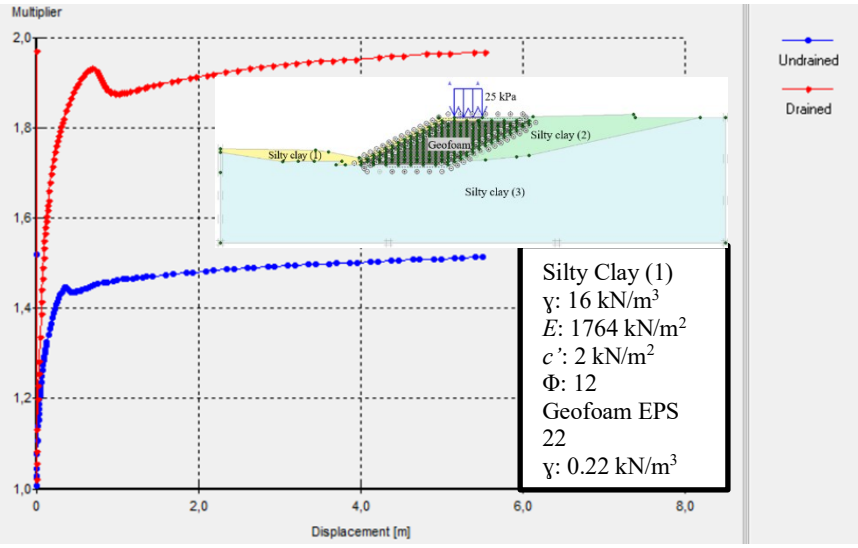

Fig. 9 Safety factor of soil with geofoam embankment (load)

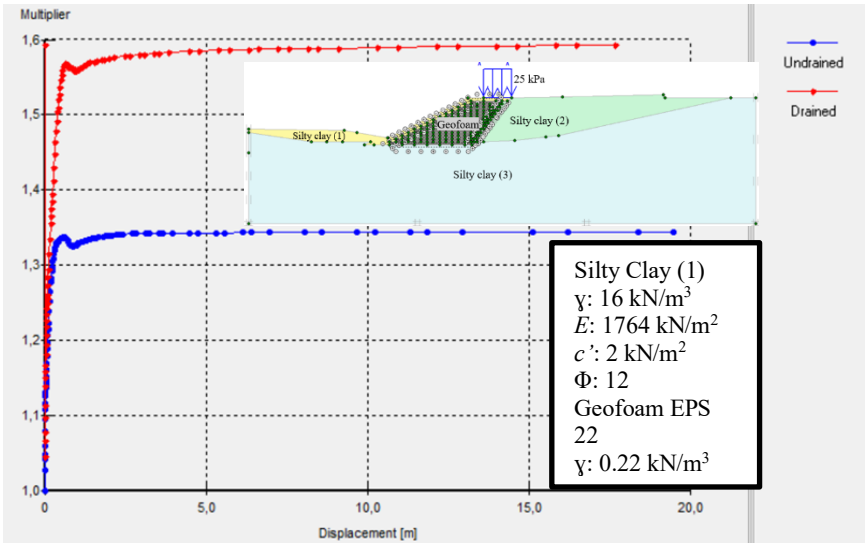

Fig. 10 Safety factor of soil with reduced geofoam embankment

3.2 Deformed mesh

For existing soil embankment, in undrained condition (Fig. 11) the largest deformed mesh elements are in the surface of silty clay (1) embankment and the maximum value of the displacement is 0.27 m ~ 27 cm. The result is little bit different with drained condition, where the maximum deformation increases to 0.31 m ~ 31 cm (Fig. 12).

Geofoam material can decrease the number of deformations. For undrained condition (Fig. 13), it decreases significantly to only 0.023 m ~ 2.3 cm. When the geofoam material is reduced (Fig. 14) to improve cost efficiency, the number of deformations increases to 0.11 m ~ 11 cm. The result is different in drained conditions, deformed number of soils with geofoam

embankment (Fig. 15) is increasing to be 0.027 m ~ 27 cm. Also, when the number of geofoam materials reduced (Fig.16), the maximum deformation will be 0.14 m ~ 14 cm. It can happen because the pore water number is reducing so that the displacement is larger than undrained condition.

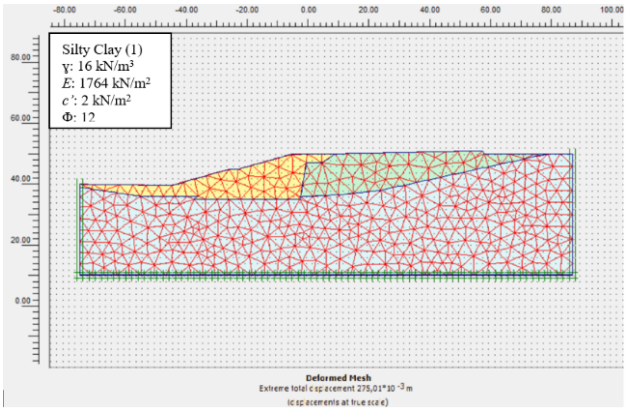

Fig. 11 Deformed mesh of existing soil embankment in undrained condition

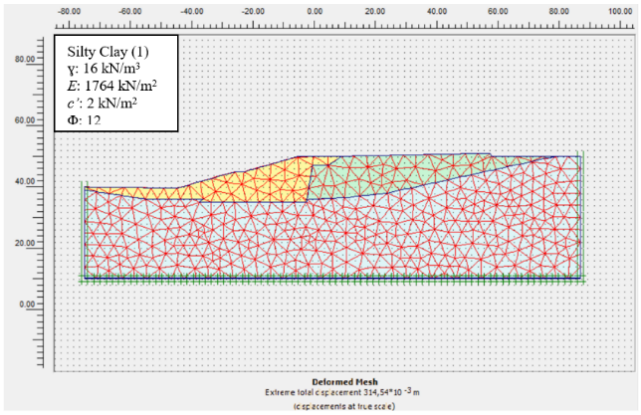

Fig. 12 Deformed mesh of existing soil embankment in drained condition

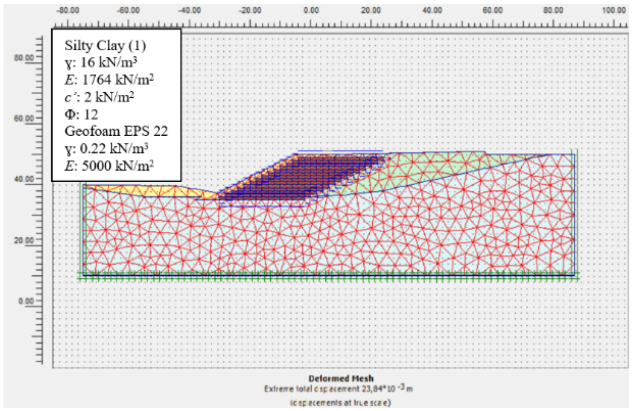

Fig. 13 Deformed mesh of soil with geofoam embankment in undrained condition

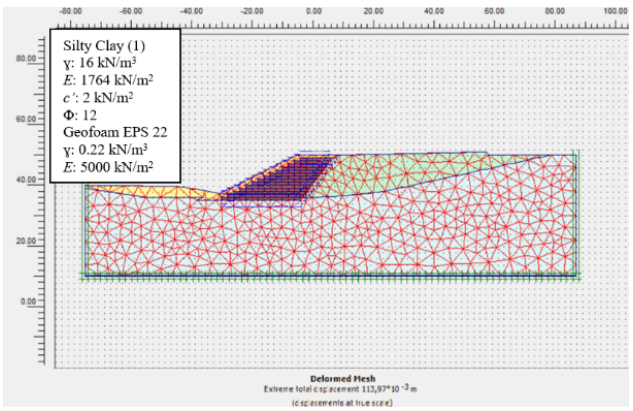

Fig. 14 Deformed mesh of soil with reduced geofoam embankment in undrained condition

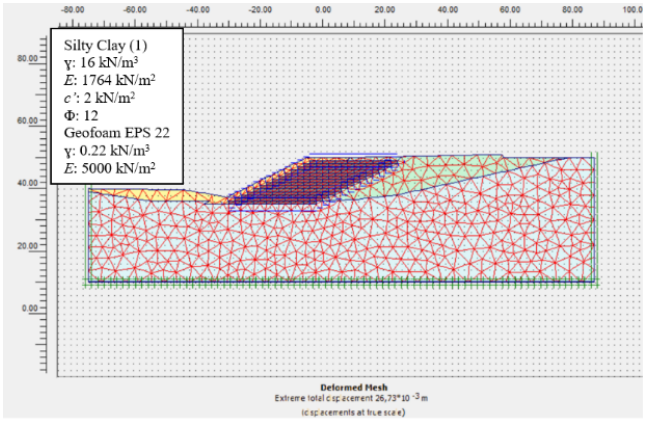

Fig. 15 Deformed mesh of soil with geofoam embankment in drained condition

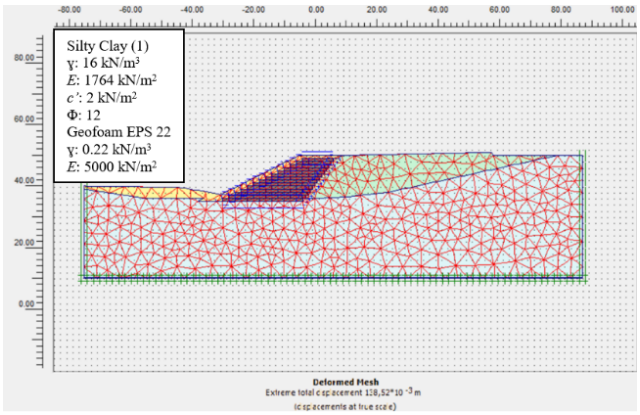

Fig. 16 Deformed mesh of soil with reduced geofoam embankment in drained condition

3.3 Total displacement

For undrained condition in existing soil (Fig. 17), the red shading of displacement indicates that the geometry The peak of the silty clay (1) slope experienced the largest displacement with a value of 0.27 m ~ 27 cm. This indicates that the potential for landslides is at the peak and its potential decreases towards the foot of the embankment. In addition, it is known that the existing silty clay soil (2) located to the right of the embankment also experienced stability disturbances in the form of displacement towards the embankment. For drained condition (Fig. 18) is not too different, but the area that has experienced displacement becomes wider, especially in the red area or maximum displacement (value: 0.31 m ~ 31 cm). This happens because of the reduced amount of pore water in the soil.

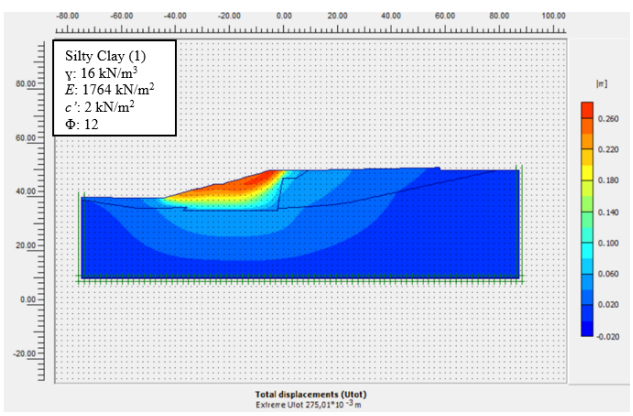

Fig. 17 Total displacement of existing soil embankment in undrained condition

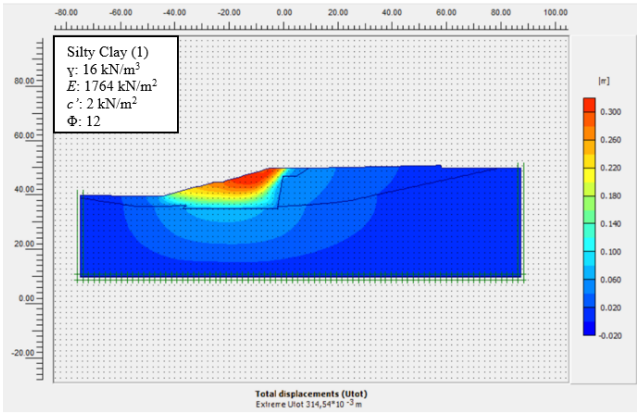

Fig. 18 Total displacement of existing soil embankment in drained condition

In soil with geofoam model, the pattern totally changing. For undrained conditions (Fig. 19) can be seen that the maximum displacement is at the upper slope tip with a total displacement of only 0.023 m ~ 2.3 cm. The displacement is indicated to be evenly distributed with very small values in silty clay (2) and silty clay (3). If the geofoam reduced 37% (Fig. 20), there is an increase in the displacement to 0.11 m ~ 11 cm. The displacement pattern is wider compared to the previous model, especially in the silty clay soil structure (2). This is because the lightweight material is not as much as in the previous model. These loads push and channel the load towards the geofoam material and have the potential for maximum displacement on the embankment slope.

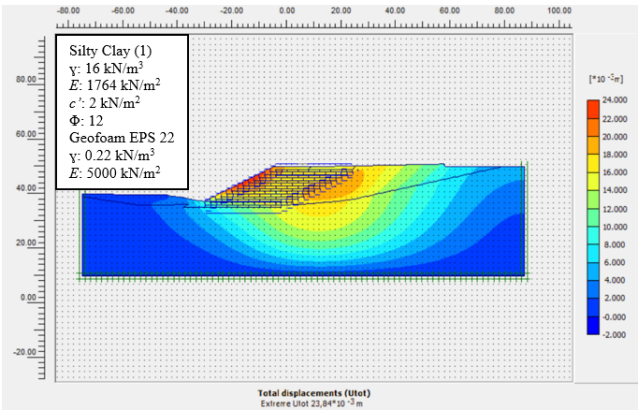

Fig. 19 Total displacement of soil with geofoam embankment in undrained condition

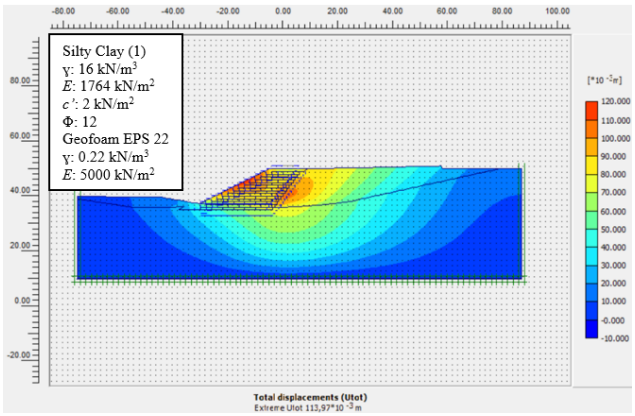

Fig. 20 Total displacement of soil with reduced geofoam embankment in undrained condition

Displacement in drained condition is always increasing, include the soil with geofoam model (Fig. 21). Where, the maximum displacement is at the highest slope tip with a value of 0.027 m ~ 2.7 cm, which is greater than the model in undrained condition. If the geofoam reduced by 37 % (Fig. 22), the value increased to 0.14 m ~ 14 cm.

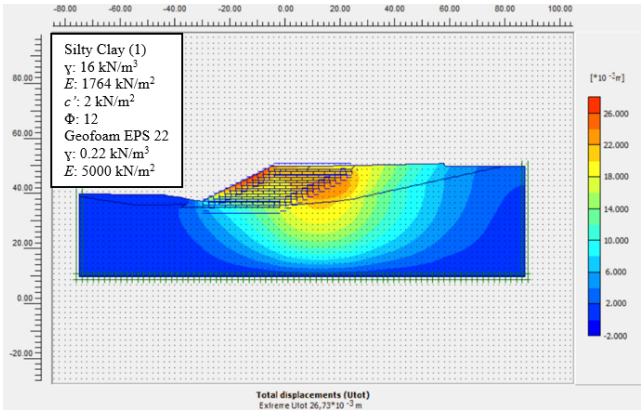

Fig. 21 Total displacement of soil with geofoam embankment in drained condition

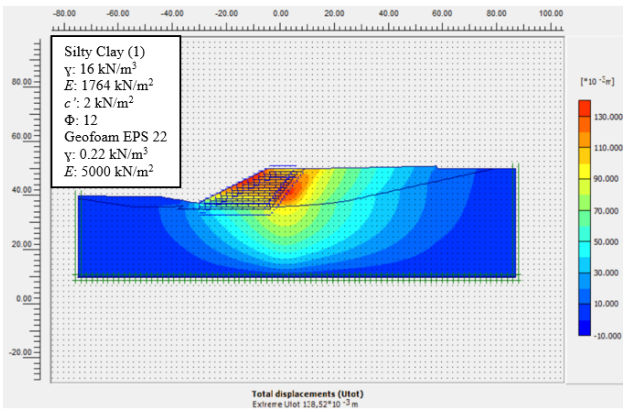

Fig. 22 Total displacement of soil with reduced geofoam embankment in drained condition

3.4 Shear strains

In the existing soil embankment in undrained condition model (Fig. 23), the shear strain due to displacement is greatest in the upper part of the silty clay slope (1) and the toe of the silty clay embankment (1) with a value of 6.41%. This indicates that the greatest deformation potential is at these two points and has the potential to experience structural failure. The drained condition (Fig. 24) shows that the failure is located at the end of the silty clay slope (1) with a value greater than the previous model, namely 5.84%.

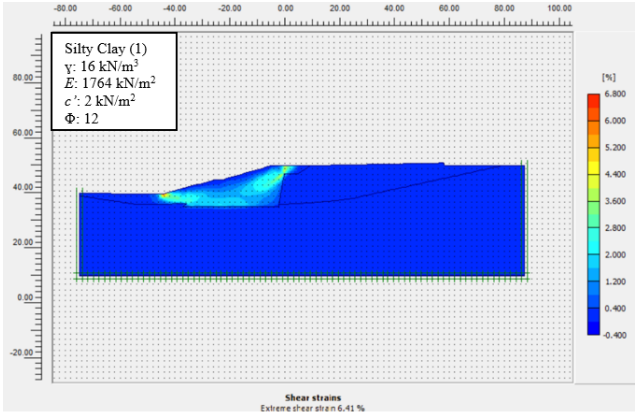

Fig. 23 Shear strain of soil embankment in undrained

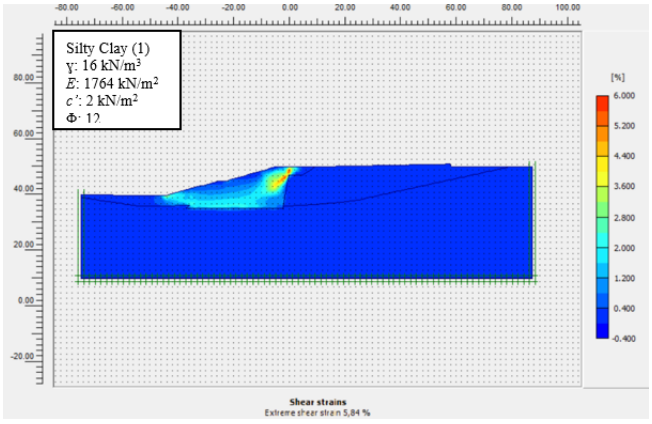

Fig. 24 Shear strain of soil embankment in drained condition

The failure in the Soil with geofoam embankment in undrained condition (Fig. 25), the shear strains in the silty clay structure (1) are the largest, precisely in the soil embankment that covers the geofoam on the slope and runs to the foot of the embankment. This indicates that the potential for failure or deformation is in the structure. However, this potential is very small, namely only around 0.35%. If the geofoam was reduced (Fig. 26), the shear strain value will increase to 2.4%. The maximum shear strain is at one point, namely at the end of the geofoam foot. This indicates that the more geofoam is used, the less potential for failure.

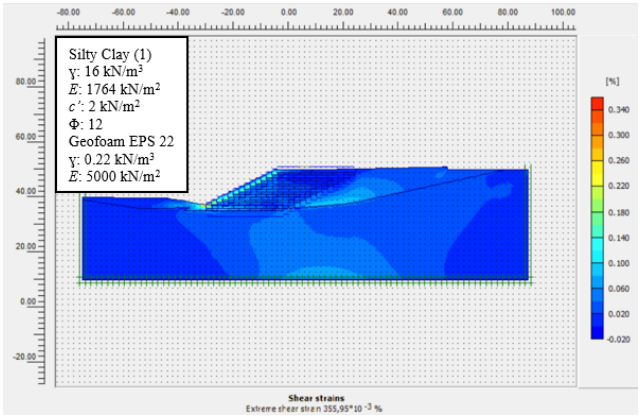

Fig. 25 Shear strain of soil with geofoam embankment in undrained condition

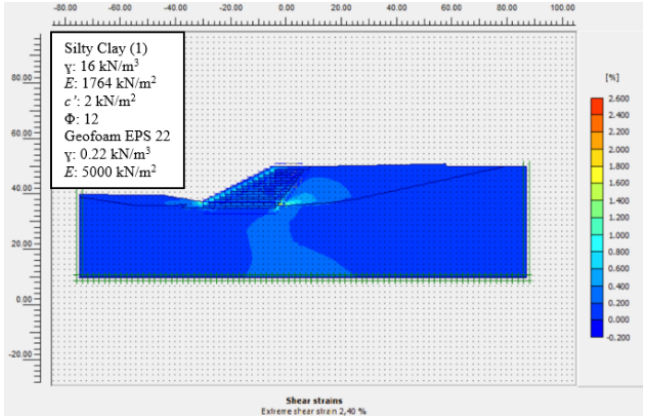

Fig. 26 Shear strain of soil with reduced geofoam embankment in undrained condition

The Soil with geofoam embankment in drained condition model (Fig. 27) shows a pattern that is almost the same as the undrained condition but the shear strains value increases to 0.34%. On the other hand, in the silty clay structure layer (2), the shear strains value increases (indicated by the shading color changing to yellow) from the undrained model. This is influenced by changes in pore water pressure so that the structure makes adjustments and produces greater deformation than the previous condition. If the geofoam material was reduced (Fig. 28) value of shear strains will increase to 2.6%, quite significant compared to the modeling without geofoam reduction. The shear strain pattern also shows that the loads originating from existing soil have a major role in the potential for shifting on geofoam slopes.

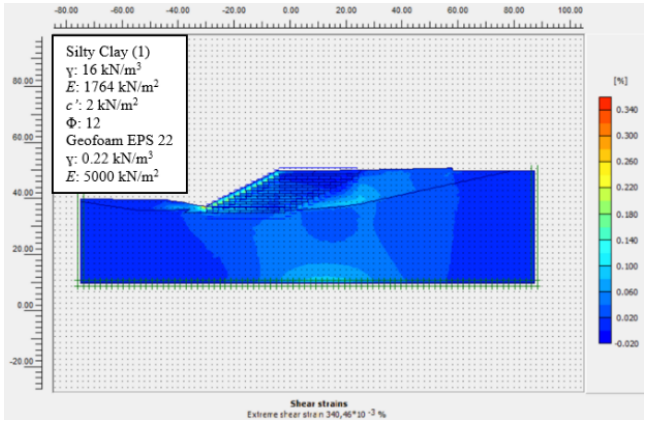

Fig. 27 Shear strain of soil with geofoam embankment in drained condition

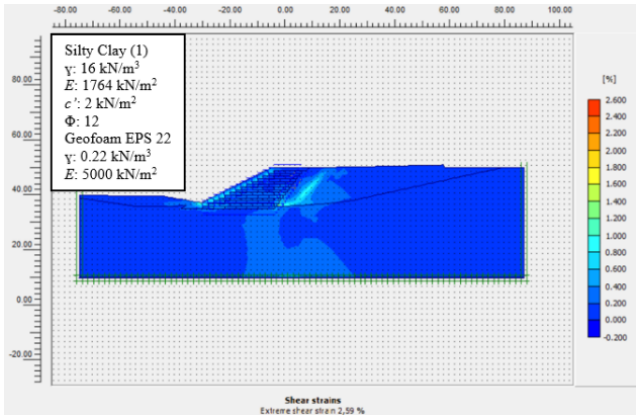

Fig. 28 Shear strain of soil with reduced geofoam embankment in undrained condition

3.5 Effective stress

Effective stress in Existing soil embankment in undrained condition model (Fig. 29) shows that the condition on the surface of the structure is the same as the value of -20 ~ 0 kN/m^2. The distribution of effective stress looks wider with extreme values found in the silty clay structure (3) which is -549.99 kN/m^2. This means that the silty clay layer (3) is the recipient of the largest structural load compared to the other 2 layers. Meanwhile, in drained condition (Fig. 30), shows a pattern that is almost the same as the previous undrained model but with a higher extreme value of -543.84 kN/m. This indicates that the pore water pressure has decreased compared to the previous model (undrained condition).

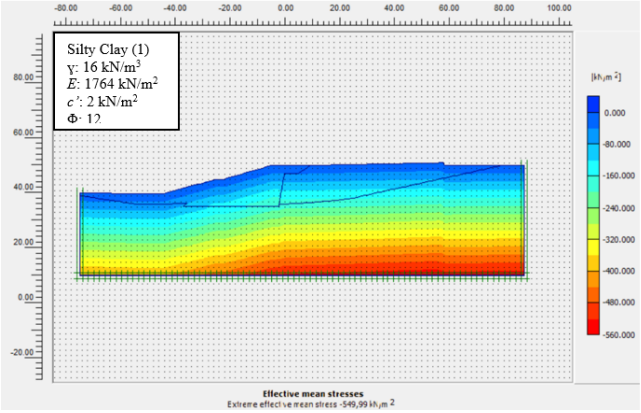

Fig. 29 Effective stress of existing soil embankment in undrained condition

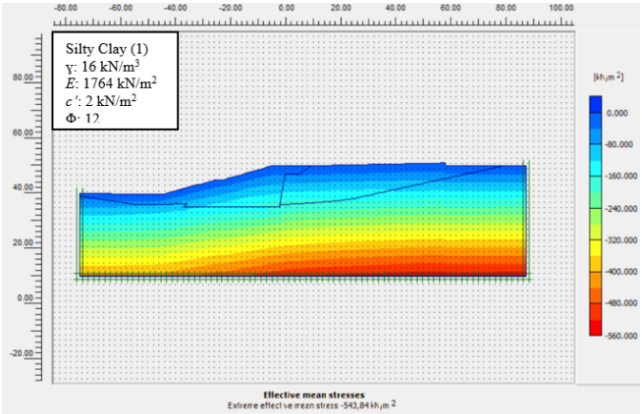

Fig. 30 Effective stress of existing soil embankment in drained condition

The next model is a soil with geofoam embankment in undrained condition (Fig. 31), where it can be seen that the effective stress on the silty clay layer (1) in the area around the geofoam and soil is more stable compared to the previous model with a value of 20 kN/m^2. Meanwhile, it can be seen that the extreme value is in the silty clay layer (3) with a value of -549.63 kN/m2 and there is no maximum value below the embankment as in the previous model. The distribution of effective stress on the slope with reduced geofoam (Fig. 32) shows that the maximum pattern (red shading) is wider compared to the previous model. This is because the load received vertically and horizontally by the base soil is increasing. The maximum effective stress value is -548.59 kN/m^2, this value is not very different compared to the value in the previous model.

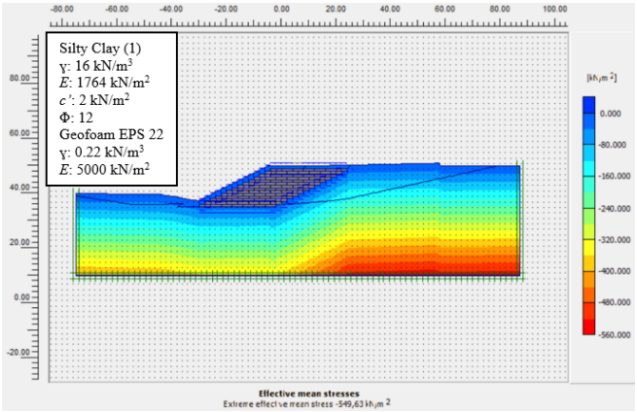

Fig. 31 Effective stress of soil with geofoam embankment in undrained condition

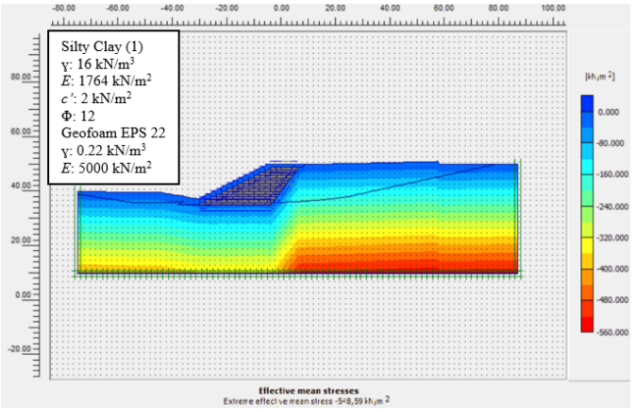

Fig. 32 Effective stress of soil with reduced geofoam embankment in undrained condition

The last comparison model, namely soil with geofoam embankment in drained condition (Fig. 33) shows a pattern that is almost the same as the model of soil with geofoam embankment in undrained condition (Fig. 34) the maximum effective stress that occurs is lower compared to the undrained condition, which is -547.69 kN/m^2. The shade pattern also shows the same thing where there is no maximum value in the silty clay layer (3) under the silty clay embankment (1), meaning that the load received on the silty clay (3) under the embankment is lighter compared to the structure without geofoam. The distribution of effective stress on the slope with reduced geofoam shows that the maximum pattern (red shading) is wider compared to the previous model which has a wider slope area with geofoam. This is because the load received vertically and horizontally by the base soil is increasing. The maximum effective stress value is -541.17 kN/m^2, this value is greater than the previous modeling value (in undrained conditions).

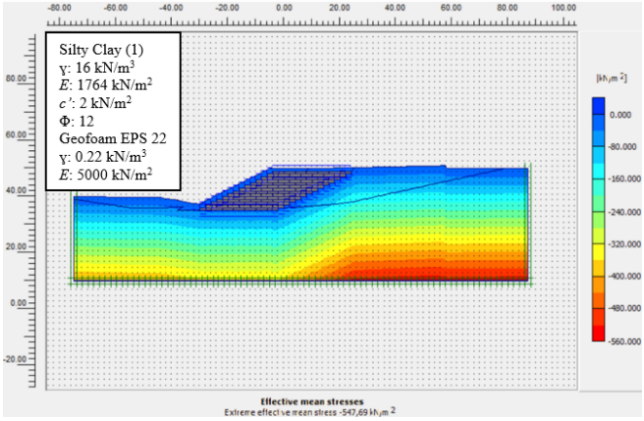

Fig. 33 Effective stress of soil with geofoam embankment in drained condition

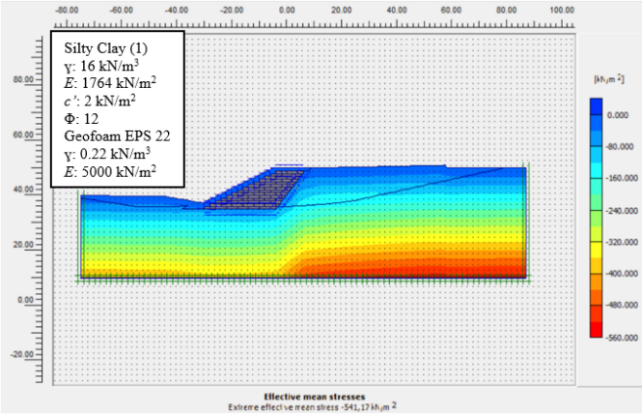

Fig. 34 Effective stress of soil with reduced geofoam embankment in drained condition

3.6 Recapitulation

To make it easier to compare each value, a recapitulation of each value will be displayed in tabular form as in Table 10.

Table 10 Recapitulation of output

Output	Models					
	Existing soil		Soil with geofoam		Soil with reduced geofoam	
	Undrained	Drained	Undrained	Drained	Undrained	Drained
Safety factors	1	1.06	1.5	1.9	1.34	1.6
Displacement (cm)	27	31	2.3	2.7	11	14
Shear strains (%)	6.41	5.84	0.35	0.34	2.4	2.6

4. Conclusions

This study purpose is to compare the displacements between soil and geofoam embankment. The results show that partial replacement of embankment soil can be replaced with geofoam. The presence of a load of 25 kPa based on SNI does not make a difference to the analysis results.

The SPT-N value can be used to become the design parameter values by performing calculations. However, this is excluded in conditions where the land has already collapsed (in the silty clay layer (1)) where the landslide conditions are caused by the parameter values. E, c', and Φ: 1764 kN/m^2, 2 kN/m^2, and 12. Different from other layers where for the SPT-N value 10: 17 kN/m^3, 8400 kN/m^2, 6 kN/m^2; and for the SPT-N value 20: 18 kN/m^3, 26880 kN/m^2, 12 kN/m^2. Because the type of soil is silty clay, the v and permeability values are the same, namely: 0.35 and 2E-9 for horizontal permeability and 1E-9 for vertical.

Displacement value of the model with geofoam is smaller than embankment without geofoam. The displacement values of the soil existing, soil with geofoam, and soil with reduced geofoam models in undrained conditions are 27 cm, 2.3 cm, and 11 cm, respectively. While in drained conditions, the values increase to 31 cm, 2.7 cm, and 14 cm. This shows that there is an effect of the amount of geofoam on the displacement value.

The results of the shear strain show that the shear failure area in embankments with geofoam is around the geofoam structure area. The deformation potential is around the area, but the percentage shows smaller results compared to the structure

without geofoam. The shear strains values in the existing soil, soil with geofoam, and soil with reduced geofoam models in undrained conditions are 6.41%, 0.35%, and 2.4%, respectively. While in drained conditions the values are 5.84%, 0.34%, and 2.6%, respectively.

Safety factors show that landslides occur on existing soil in undrained conditions because the SF value = 1. Furthermore, in drained conditions, SF increases but is not significant to 1.06, and the value does not meet the standard. Using the landslide soil parameters, a comparison is made with the geofoam structure, where it is found that the SF value = 1.5 in undrained conditions and increases to 1.9 in drained conditions. This value is SF > 1.25 which is required by SNI so that the slope condition is stable. Adjustments for cost reduction were made back to the soil embankment with geofoam embankment, namely by reducing the amount of geofoam by 37%, it was found that the SF in undrained conditions was 1.34 and 1.6 in drained conditions.

Acknowledgments

The author would like to express sincere gratitude to Dr. Ir. Eddy Triyanto Sudjatmiko, S.T., M.T. for his invaluable guidance and supervision throughout the process of compiling this study, which has culminated in the publication of this paper. The author also extends appreciation to all the lecturers whose knowledge and insights contributed to the preparation of this manuscript. Heartfelt thanks are also directed to Beasiswa Pendidikan Indonesia for their financial support through the LPDP and Kemendikbudristek, which made this research possible. Without such support, the completion of this research would not have been feasible. It is hoped that the findings of this study will make a meaningful contribution to the advancement of science and research.

References

[1] N. Andajani and Y. Risdianto., "Penambahan Kapur sebagai Stabilitas Tanah Ekspansif untuk Lapisan Tanah Dasar (Subgrade)," Publikasi Riset Orientasi Teknik Sipil (Proteksi), vol. 4, no. 2, pp. 90-95, 2022.

[2] P. Kevin, "Lightweight Embankment: Performance Comparison of Geofoam and Mortar Busa for Settlement Reduction and Stabilization of Embankment over Soft Soil," in 27th Annual National Conference on Geotechnical Engineering, pp. 296-303, Jakarta, Indonesian Society for Geotechnical Engineering (ISGE), 2023.

[3] A. Faishol, L. Wijayanti, and M. Mulyadi, "Inovasi Struktural: Pemanfaatan Geofoam Expanded Polystyrene (Eps) Dalam Pembangunan Infrastruktur Modern," Jurnal Teknik Sipil Universitas 17 Agustus 1945 Semarang, vol. 17, no. 01, pp. 46-61, 2024.

[4] Geofoam International, "Standard Sized EPS Geofoam Blocks," Geofoam International LLC. Available: https://geofoamintl.com/products/standard-sized-geofoam-blocks/. [Accessed: Apr. 3, 2025].

[5] Geofoam Research Center, "Slope Stabilization," Geofoam Research Center, Syracus University. Available: http://geofoam.syr.edu/slope-stabilization.html. [Accessed: Apr. 3, 2025].

[6] A. Gunawan, "Geofoam: A Potential for Indonesia's Soil Problem II," in 4th International Conference on Eco Engineering Development 2020, pp. 1-7, Florida, 240th ECS Meeting, 2021.

[7] E. T. Sudjatmiko, "Penelitian Karakteristik Parameter Kuat Geser Tanah Lempung Ekspansif Cikarang dengan Uji Laboratorium dan Uji Insitu," Ph.D. dissertation, Universitas Katolik Parahyangan, Bandung, 2017.

[8] E. T. Sudjatmiko, "SPT and CPT Correlation of Expansive Clay in Cikarang, Indonesia," Journal of the Civil Engineering Forum, pp. 245-256, 2022.

[9] S. Giovanni, I. B. Mochtar, and N. Endah, "Usulan Penyelesaian Masalah Rekayasa Tanah untuk Jalan dan Gedung di Atas Tanah Ekspansif Studi Kasus Surabaya Barat," Jurnal Teknik ITS, vol. 7, no. 1, pp. 186-191, 2018.

[10] J. H. Schmertmann, "Static Cone to Compute Static Settlement Over Sand," Proceedings of the American Society of Civil Engineers, pp. 1011-1133, Florida, Journal of the Soil Mechanics and Foundations Division, 1970.

[11] J. E. Bowles, Foundation Analysis and Design, 5th ed., The McGraw-Hill Companies, Inc., 1993.

[12] M. M. Rahman, Foundation Design using Standard Penetration Test (SPT) N-value, Bangladesh: Bangladesh Water Development Board, 2020.

[13] Y. P. A. Rumbyarso and G. Pribadi, "Penggunaan Program Plaxis Dalam Studi Penelitian Perkuatan Geotextile pada Kestabilan Lereng Buatan," Jurnal Sipil Krisna, vol. 9, no. 1, pp. 22-26, 2023.

[14] M. P. Hibatulloh and I. N. Hamdan, "Permodelan Penanganan Longsoran Lereng dengan Perkuatan Dinding Penahan Tanah di Kawasan Artha Industrial Hills-Karawang Menggunakan Plaxis 2D," FTSP Series: Seminar Nasional dan Diseminasi Tugas Akhir 2023, pp. 335-340, Bandung, National Technology Institute, 2023.

[15] M. T. Simanjorang and Hendriyawan, "Desain dan Analisis Timbunan untuk Keperluan Reklamasi Menggunakan Metode Elemen Hingga," Bandung, Prodi Teknik Kelautan, Fakultas Teknik Sipil dan Lingkungan, Institut Teknologi Bandung, 2021.

[16] E. Widjaja, N. Ivana, and R. J. Nur, "Analisis Stabilitas Jangka Pendek dan Jangka Panjang Timbunan Tanah Lunak Menggunakan Tipe Drainase Undrained A dan Undrained B pada Metode Elemen Hingga Plaxis 2D," Syntax Idea, vol. 5, no. 9, pp. 1144-1156, 2023.

[17] I. Hidayat and A. Suhendra "Aplikasi Geofoam sebagai Material Timbunan di Atas Tanah," ComTech, vol. 2, no. 1, pp. 106-116, 2011.

[18] J. S. Horvath, "The Compressible-Inclusion Function of EPS Geofoam: Analysis and Design Methodologies," Geotextiles and Geomembrane, pp. 77-120, 1997.

[19] P. P. Rahardjo, B. W. Anggoro, M. Wijaya, and D. P. Seourin, "EPS-Geofoam as Lightweight material for Replacement of Embankment Fill to Overcome Landslide Problems at STA 40+200 of Cisumdawu Toll Road, West Java," IOP Conf. Series: Earth and Environmental Science, pp. 1-21, 2023.

[20] D. K. Srivastava, A. Srivastava, A. K. Misra, and V. Sahu, "Sustainability Assessment of EPS-Geofoam in Road Construction: A Case Study," International Journal of Sustainable Engineering, pp. 1-8, 2018.

[21] H. Tanada, A. Handoko, and P. P. Rahardjo, "The Use of Lightweight Material at Road Access Construction on Slope," Indonesian Geotechnical Journal, vol. 2, no. 3, pp. 95-108, Dec. 2023.